Published in final edited form as:
Biomaterials. 2009 December ; 30(36): 6844–6853. doi:10.1016/j.biomaterials.2009.08.058.

Thermosensitive injectable hyaluronic acid hydrogel for adipose tissue engineering

Huaping Tan[1], **Christina M. Ramirez**[1], **Natasa Miljkovic**[1], **Han Li**[1], **J. Peter Rubin**[1,2], and **Kacey G. Marra**[1,2,3,*]

[1] Division of Plastic Surgery, Department of Surgery, University of Pittsburgh; Pittsburgh, PA

[2] McGowan Institute for Regenerative Medicine, University of Pittsburgh, Pittsburgh, PA

[3] Department of Bioengineering, University of Pittsburgh, Pittsburgh, PA

Abstract

A series of thermosensitive copolymer hydrogels, aminated hyaluronic acid-g-poly(*N*-isopropylacrylamide) (AHA-g-PNIPAAm), were synthesized by coupling carboxylic end-capped PNIPAAm (PNIPAAm-COOH) to AHA through amide bond linkages. AHA was prepared by grafting adipic dihydrazide to the HA backbone and PNIPAAm-COOH copolymer was synthesized via a facile thermo-radical polymerization technique by polymerization of NIPAAm using 4,4′-azobis(4-cyanovaleric acid) as an initiator, respectively. The structure of AHA and AHA-g-PNIPAAm copolymer was determined by ^{1}H NMR. Two AHA-g-PNIPAAm copolymers with different weight ratios of PNIPAAm on the applicability of injectable hydrogels were characterized. The lower critical solution temperature (LCST) of AHA-g-PNIPAAm copolymers in PBS were measured as ~30°C by rheological analysis, regardless of the grafting degrees. Enzymatic resistance of AHA-g-PNIPAAm hydrogels with 28% and 53% of PNIPAAm in 100U/mL hyaluronidase/PBS at 37°C was 12.3% and 37.6% over 28 days, respectively. Equilibrium swelling ratios of AHA-g-PNIPAAm hydrogels with 28% of PNIPAAm were 21.5, and significantly decreased to 13.3 with 53% of PNIPAAm in PBS at 37°C. Results from SEM observations confirm a porous 3D AHA-g-PNIPAAm hydrogel structure with interconnected pores after freeze-drying and the pore diameter depends on the weight ratios of PNIPAAm. Encapsulation of human adipose-derived stem cells (ASCs) within hydrogels showed the AHA-g-PNIPAAm copolymers were noncytotoxic and preserved the viability of the entrapped cells. A preliminary *in vivo* study demonstrated the usefulness of the AHA-g-PNIPAAm copolymer as an injectable hydrogel for adipose tissue engineering. This newly described thermoresponsive AHA-g-PNIPAAm copolymer demonstrated attractive properties to serve as cell or pharmaceutical delivery vehicles for a variety of tissue engineering applications.

1. Introduction

Hydrogels have been recognized as having a variety of applications in drug delivery, tissue engineering and regenerative medicine [1–2]. Injectable hydrogels have been extensively explored as cell delivery systems with the advantage that cells and biomolecules can be readily integrated into the gelling matrix [3–4]. The injectable nature of the hydrogels provides the

*To whom all correspondence should be addressed: Kacey G. Marra, PhD, Department of Surgery, 1655E Biomedical Science Tower, 200 Lothrop Street, University of Pittsburgh, Pittsburgh, PA 15261, 412-383-8924, 412-648-2821 (fax), marrak@upmc.edu.

attractive feature of facile and homogenous cell distribution within any defect size or shape prior to gelation. In addition, injectable hydrogels allow good physical integration into the defect, potentially avoiding an open surgery procedure and facilitating the use of minimally invasive approaches for material delivery [5–6].

Injectable, biodegradable hydrogels capable of phase transition in response to external stimuli such as temperature represent another type of useful building blocks for biomedical applications [7–8]. Thermoresponsive phase transition has been realized for potential tissue regeneration because gelation can be realized simply as the temperature increases above the lower critical solution temperature (LCST), which is designed to be below body temperature [9–12]. Poly(*N*-isopropylacrylamide) (PNIPAAm) is a typical paradigm of thermosensitive polymers that undergo a coil-to-globule phase transition ~32 °C [13–14]. The thermosensitivity of hydrogels can be achieved by incorporating PNIPAAm into the backbone of biodegradable polymers. Over the past decade, various thermosensitive and injectable polymers including poly(ethylene oxide), chitosan, gelatin, hyaluronic acid, and PNIPAAm copolymers have been developed and employed in a variety of settings [15–18]. For example, Cho et al. [17] synthesized chitosan-g-PNIPAAm copolymer, and determined that human mesenchymal stem cells (MSCs) could undergo chondrogenesis when the copolymer was used as a thermosensitive cell-polymer complex. Ha et al. [18] reported that the PNIPAAm-grafted hyaluronic acid copolymer was prepared to create temperature-sensitive injectable gels for use in controlled drug delivery applications. From the *in vitro* riboflavin release study, the PNIPAAm-grafted hyaluronic acid gel showed a more sustained release behavior when the grafting yield of PNIPAAm onto the HA backbone was increased. In addition, thermosensitive NIPAAm-based hydrogels can be synthesized by copolymerization of NIPAAm with other monomers such as acrylic acid, *N*-hydroxysuccimide and polylactide-hydroxyethyl methacrylate [19]. Moreover, Ohya et al. [20–21] have developed a photopolymerization method to synthesize PNIPAAm-gelatin and PNIPAAm-hyaluronic acid polymers for applied as cartilage regeneration and tissue adhesion prevention materials.

Hyaluronic acid (HA) is a naturally non-sulfated glycosaminoglycan that is widely distributed throughout the extracellular matrix (ECM) of all connective tissues in human and other animals [22–23]. HA is an enzymatically degradable glycosaminoglycan consisting of multiple repeating disaccharide units of *N*-acetyl-*D*-glucosamine and *D*-glucuronic acid. HA plays an important role in many biological processes such as tissue hydration, nutrient diffusion, proteoglycan organization, and cell differentiation. Due to its good biocompatibility, biodegradability, as well as excellent gel-forming properties, hyaluronic acid shows promise in biomedically-relevant hydrogel systems. In addition to the above thermosensitive copolymers, other injectable hyaluronic acid hydrogels have been developed using various methods, including photopolymerization [24–25], Michael addition crosslinking [26–27], Schiff-base reaction crosslinking [28–29], and covalently crosslinking with chemical agents [30]. Our objective in this work was to synthesize an injectable hyaluronic acid hydrogel that would be appropriate for soft tissue cell therapy applications. Specifically, we desired a bioactive material that would be readily injectable at or below room temperature, would maintain its bioactivity and support cell survival, and would form a gel with relatively appropriate biodegradable properties under physiological conditions.

An effective method to combine the PNIPAAm with biodegradable polymers is copolymerization by free radical polymerization using 2,2-azobisisobutyronitrile (AIBN), benzyl peroxide (BPO) and ammonium persulfate (APS) as initiators [31–33]. The procedure is to synthesize a carboxyl- or amino-terminated NIPAAm copolymer, which is then coupled onto biomacromolecular or peptide sequences. A convenient approach to synthesize carboxyl-terminated PNIPAAm (PNIPAAm-COOH) using 4,4′-azobis(4-cyanovaleric acid) as an initiator has been used to prepare thermosensitive gene vectors [34–35]. In this study, we put

forward this method to broaden thermosensitive hydrogel system. Hyaluronic acid was aminated and partially grafted with PNIPAAm-COOH, in which the desired degree of grafting are obtained under mild reaction conditions. The effects of the PNIPAAm ratio on LCST, enzymatic biodegradability, swelling, and biological properties of the resulting copolymers were examined. The potential application of the thermoresponsive hyaluronic acid as a functional injectable scaffold in soft tissue engineering was studied by encapsulation behavior of human adipose-derived stem cells (ASCs). A preliminary *in vivo* study of the injectable efficacy in the thermoresponsive hyaluronic acid gel is also reported.

2. Materials and methods

2.1. Materials

Chemicals were purchased from Sigma-Aldrich unless otherwise stated. *N*-isopropylacrylamide (NIPAAm) was purified by recrystallization in ethyl acetate and hexane respectively before use. Hyaluronic acid sodium (molecular weight, ~1.6×10^6), adipic dihydrazide (ADH), 1-ethyl-3-(3-dimethylaminopropyl) carbodiimide hydrochloride (EDC), 1-hydroxybenzotriazole hydrate (HOBt), 4,4′-azobis(4-cyanovaleric acid) (ACA) and trinitrobenzenesulfonic acid (TNBS) were used as received. CyQuant Cell Proliferation Assay Kit was purchased from Invitrogen, Eugene, Oregon, USA.

2.2. Synthesis of AHA

AHA was synthesized in aqueous conditions following previously described procedures with slight modifications [33,35]. Briefly, 0.5g of HA was dissolved in 100mL nanopure H_2O to result in a 5 mg/ml solution. 10g of ADH was added to this HA solution. 0.8g of EDC and 0.7g HOBt were dissolved in DMSO/H_2O (1:1 v/v, 5ml each) and added to the reaction mixture. The pH of the solution was adjusted to 5.0 by adding 1*N* HCl. The reaction was stirred for 24h at room temperature and then was exhaustively dialyzed (MWCO 10000, Spectra/Por membrane, Rancho Dominguez, CA, USA) against nanopure H_2O for 3 days. NaCl was then added to produce a 5% (w/v) solution and the AHA was precipitated in ethanol. The precipitate was re-dissolved in H_2O and dialyzed for 3 days to remove the salt. The purified product was freeze dried at −50°C (Freezone 4.5, Labconco US) and kept at 4°C. The structure of AHA was determined by ^{1}H NMR (300 MHz, Bruker Avance) spectra at ambient temperature using D_2O as a solvent. The percentage of hydrazide group substitution in the AHA polymer was quantified as 64% using a TNBS assay [36].

2.3. Synthesis of PNIPAAm-COOH

PNIPAAm-COOH was synthesized as described previously [34–35]. In brief, 5g NIPAAm and 60mg ACA were dissolved in 25ml methanol to form a 20 wt % monomer solution. The solution was bubbled with a nitrogen atmosphere for 10 min and incubated at 68°C for 3h. The solution was then dropped into hot water (60°C) to precipitate the PNIPAAm-COOH. After washed two times with hot water, the polymers were dissolved in nanopure water (20°C), and then lyophilized (−50°C). The number-average molecular weight (Mn, 1.12×10^4Da) and polydispersity index (1.39) were determined by gel permeation chromatography (GPC, Waters Mode 515 HPLC pump, Milford, MA, USA) with phenogel 10^4, 500 Å columns and refractive index detector using tetrahydrofuran (THF) as a mobile phase. Monodisperse polystyrenes were used as standards.

2.4. Synthesis of AHA-g-PNIPAAm

AHA-g-PNIPAAm copolymers were synthesized by grafting PNIPAAm-COOH onto AHA chain as shown in Scheme 1. 0.5g of AHA was dissolved in 200mL nanopure H_2O to make a solution. To graft the PNIPAAm-COOH onto AHA, PNIPAAm-COOH was dissolved in

nanopure H_2O and incubated with EDC at 4°C for 48h. The PNIPAAm-COOH/EDC amounts were varied with 0.5g/0.1g and 1g/0.2g to fabricate two AHA-g-PNIPAAm copolymer samples with different PNIPAAm grafting degrees. The PNIPAAm-COOH/EDC solution was then added into the AHA solution under agitation with a final pH value of 5.6. The mixture was incubated at room temperature for 24h before dialysis (MWCO 25,000) for several days. The dialyzed water became turbid upon heating, illustrating the successful separation of the unreacted PNIPAAm-COOH. To verify the AHA-g-PNIPAAm copolymer structure, ^1H NMR spectra were measured at ambient temperature using D_2O as a solvent. The remaining hydrazide groups were also tested by the TNBS method to estimated weight ratios of grafting PNIPAAm.

2.5. Rheological analysis

AHA-g-PNIPAAm copolymers were dissolved in PBS (pH = 7.4) to form a solution with a concentration of 5 wt %. The sol-gel transition of the copolymer aqueous solutions was investigated using a strain-controlled rheometer (AR2000, TA instrument, USA) and a parallel plate (diameter, 40 mm). The heating rate was set at 0.5°C/min, while the angular frequency ω was set at 6.283 rad/s.

2.6. Characterization of AHA-g-PNIPAAm hydrogels

2.6.1. In vitro enzymatic degradation—Degradation of hydrogels was examined with respect to weight loss under aqueous conditions in the presence of hyaluronidase. Hyaluronidase was dissolved in PBS to result in a 100 U/mL enzyme solution. 5 wt % of AHA-g-PNIPAAm copolymer solution in PBS was placed in a 37°C water bath for 15 min to allow gelation. Initially dry hydrogels were weighed (W_0) after quickly frozen at −80°C and lyophilized at −50°C. Weight loss of dry hydrogels was monitored as a function of incubation time in PBS or enzyme solution at 37°C. At specified time intervals, hydrogels were quickly frozen at −80°C, lyophilized and weighed (W_t). The weight loss ratio was calculated as $100\% \times (W_0 - W_t)/W_0$. The weight remaining ratio was defined as $1 - 100\% \times (W_0 - W_t)/W_0$.

2.6.2. Equilibrium swelling—The equilibrium swelling of AHA-g-PNIPAAm copolymer hydrogels were measured in PBS and DMEM/F12/10%FBS (heat-inactivated fetal bovine serum) at 37°C. 5 wt % of AHA-g-PNIPAAm copolymer solution in PBS was placed in a 37°C water bath for 15min to allow gelation. The hydrogel was immersed in PBS or DMEM/F12/10%FBS and kept at 37°C for 4 h until equilibrium of swelling had been reached. The swollen hydrogels were removed from incubation medium, wiped with tissue paper to remove the surface water at 37°C and weighed immediately (Ws). Dry hydrogels were weighed (Wd) after quickly frozen at −80°C and lyophilized. The equilibrium swelling ratio (ESR) was calculated using the following equation: $ESR = (Ws - Wd)/Wd$.

2.6.3. Hydrogel morphologies—Morphologies of AHA-g-PNIPAAm copolymer hydrogels were observed by utilizing scanning electron microscopy (SEM). The hydrogels were immersed into liquid nitrogen and freeze-dried at −50°C. The cross-section of hydrogels were gold-coated using a Cressington 108 Auto (Cressington, Watford UK) and viewed using a JSM-6330F SEM (JEOL, Peabody, MA) operated at 10kV accelerating.

2.7. Cell culture

Human adipose-derived stem cells (ASCs) were isolated from human adipose tissue obtained from elective cosmetic surgery procedures performed at the University of Pittsburgh [37–38]. The fat tissues were minced with scissors in the collagenase solution consisted of Hanks' balanced salt solution (3.0 mL/g of fat) (Sigma-Aldrich, St. Louis, MO), bovine serum albumin (fatty acid free, pH 7.0, 3.5 g/100 mL Hanks') (Intergen Company, Purchase, NY) and 1% type

II collagenase (3.0 mg/g of fat) (Worthington Biochemical Corporation, Lakewood, NJ). The centrifuge tubes were shaken at 100 rpm for 50 min at 37°C. Following digestion, the content of each tube was filtered through double-layered sterile gauze. The filtrates were then centrifuged at 1000 rpm for 10 min at 37°C, and a three layer suspension, consisting of a fatty layer on the top, a serum layer in the middle, and a cellular pellet at the bottom of each tube, was obtained. The fatty layer and most of the supernatant was aspirated off, leaving the pellet intact at the bottom. The pellet in each tube was then suspended in 10 mL of erythrocyte lysis buffer (pH = 7.4), vortexed, and centrifuged again at 1000 rpm for 10 min at 37°C. The pellets were suspended in the plating medium consisted of DMEM/F12 with 10% heat-inactivated fetal bovine serum, 1% penicillin/streptomycin and 1% Fungizone (all products obtained from Gibco, Invitrogen Corporation, Carlsbad, CA). Adherent ASCs were expanded for a period of 5–8 days at 37°C, and the medium was changed every other day until the cells achieved 80% confluence.

Encapsulation of ASCs within AHA-g-PNIPAAm copolymer hydrogel was evaluated. Dry AHA-g-PNIPAAm copolymer was sterilized under UV irradiation in the laminar flow hood for 60 min and then dissolved in sterilized PBS at room temperature to obtain 5 wt% solution. The AHA-g-PNIPAAm solution was chilled to 0°C and exposed to UV irradiation for another 30 min. 5mL of AHA-g-PNIPAAm solution was added into a centrifugal tube containing 25×10^6 ASCs. The final cell density was 5×10^6/mL copolymer solution. After sufficient mixing, the cell containing solutions were injected into 48-well culture plate and incubated at 37°C to form hydrogels (300 μL/well). After 15 min, pre-warmed DMEM/F12/10%FBS medium (37°C) was added into each well and changed daily.

2.8. Cytoviability assay

The cell numbers in the AHA-g-PNIPAAm copolymer hydrogels were determined by measuring the amount of DNA. Samples were frozen at −80°C for 4 h, and lyophilized for 24 h. The DNA content was quantified using a CyQuant Cell Proliferation assay [37]. The live/dead cells were observed by confocal laser scanning microscopy (CLSM, Olympus FV1000). The live cells were dyed with fluorescein diacetate (FDA, Green) and dead cell nuclei were dyed with propidium iodide (PI, Red). The details of encapsulated cell/gel matrices were further observed by SEM. The cultured cell/gel matrices were rinsed in PBS, fixed with 2.5 % glutaraldehyde for 60 min, and dehydrated in a graded series of alcohols at 37°C. The matrices were observed after air drying and gold coating.

2.9. In vivo model

A 5 wt % AHA-g-PNIPAAm copolymer hydrogel in PBS was administered by dorsal subcutaneous injections in male athymic nude mice (n=6, 6 week-old, Harlan, Indianapolis, Ind.) to evaluate biocompatibility *in vivo*. Each injection was 1 ml in volume and performed through hypodermic syringe. For histological evaluation, animals were sacrificed and excised gel-implants were rinsed in PBS and fixed in 10 % buffered formalin at 37°C. The gel-explants and surrounding tissues were dehydrated in a graded series of alcohols at 37°C, and embedded in paraffin. The transverse paraffin was sectioned through the center of gel-implants at 5-μm thickness, and histologically processed using hematoxylin and eosin (H & E) stains.

This study was conducted in accordance with the regulations of the Human Studies Committee of the University of Pittsburgh. Tissue collection was performed according to a protocol approved by the University of Pittsburgh Institutional Review Board.

2.10. Statistical analysis

The experimental data from all the studies were analyzed using Analysis of Variance (ANOVA). Statistical significance was set to p value ≤ 0.05. Results are presented as mean ± standard deviation.

3. Results and discussion

3.1. Synthesis and characterization of AHA-g-PNIPAAm copolymer

Following the synthesis routes shown in Scheme 1, AHA-g-PNIPAAm copolymers were successfully obtained, as determined by the ^{1}H NMR spectra with evidence of proton peaks from the ADH residue (a, b and c) and NIPAAm residues (d, e, f and g) (Fig. 1). Fig. 1a shows the ^{1}H NMR spectrum of AHA. A peak at 1.9 ppm was assigned to the acetamido moiety of the *N*-acetyl-D-glucosamine residue of HA, and the peaks between 2.2–2.4 ppm refer to the integration of methylene protons of ADH [29]. A typical spectrum of AHA-g-PNIPAAm copolymer (Fig. 1b) presents both the resonance peaks from ADH and PNIPAAm, demonstrating the occurrence of the grafting reaction. As shown in spectrum, the peaks at 1.1 and 3.9 ppm are assigned to $–CH_3$ and –NH– group, respectively [35]. The estimated weight ratios of PNIPAAm in the AHA-g-PNIPAAm copolymers were 28% and 53% varied with the feeding amount of 0.5g/0.1g and 1g/0.2g PNIPAAm-COOH/EDC, respectively. For brevity, the AHA-g-PNIPAAm copolymers are designated as AHA-g-PNIPAAm-28 and AHA-g-PNIPAAm-53, respectively.

3.2. Rheological analysis

The kinetics of AHA-g-PNIPAAm copolymer hydrogel formation were measured by monitoring the viscosity and storage modulus (G′) as a function of temperature. The viscosity and storage modulus of AHA-g-PNIPAAm-28 and AHA-g-PNIPAAm-53 in PBS as a function of temperature are shown in Fig. 2. At temperatures > 30°C, the viscosity and storage modulus values increased rapidly. The transition from liquid-like behavior to elastic gel-like behavior occurs which was observed at approximately ~30°C. The viscosity and storage modulus quickly leveled off after 32°C, indicating that the network structure of the hydrogels was completed through dehydration of PNIPAAm chain. The viscosity and storage modulus of the AHA-g-PNIPAAm-53 were higher than those of the AHA-g-PNIPAAm-28 due to the stronger dehydration interaction. The insets in Fig. 2a demonstrate the sol-gel reversibility of the AHA-g-PNIPAAm-53 hydrogel in PBS. The sol-gel transition of the AHA-g-PNIPAAm-53 solutions occurred within 1 minute with increased temperature. The copolymer solution became opaque and formed a stable hydrogel *in situ* at 37°C. This fast sol-to-gel phase transition behavior is beneficial for cell entrapment to give a uniform distribution of cells within the gelled matrix [33].

Both of the AHA-g-PNIPAAm-28 and AHA-g-PNIPAAm-53 solutions reveal reversible soluble-insoluble characteristics with respect to temperature change. By defining the LCST observed in a heating process as the gel formation temperature, the sharp thermo-precipitation curves show that the LCST of AHA-g-PNIPAAm-28 and AHA-g-PNIPAAm-53 were ~30°C. The grafted ratio of PNIPAAm demonstrates no influence on the phase transition behavior of copolymer. The LCST of the PNIPAAm is ~32°C, which can be altered by copolymerizing NIPAAm with hydrophilic polymer and other monomers [20,33]. In the AHA-g-PNIPAAm copolymer hydrogel, the hydrophilic HA backbone prevents the dehydration of the PNIPAAm chains and expands the collapsed structure above LCST.

3.3. Characterization of AHA-g-PNIPAAm hydrogels

The weight loss and enzymatic resistance of two AHA-g-PNIPAAm copolymer hydrogels were monitored as a function of incubation time in PBS at 37 °C (Fig. 3). The grafting ratio of PNIPAAm has a significant influence on the weight loss behavior of copolymer hydrogels. The AHA-g-PNIPAAm-28 hydrogels showed a significantly faster weight loss rate than the AHA-g-PNIPAAm-53 hydrogels in PBS after 14d incubation ($p < 0.05$). At day 28, the weight remaining ratio of AHA-g-PNIPAAm-28 and AHA-g-PNIPAAm-53 hydrogels were 63.1% and 79.4%, respectively. HA is an enzymatically degradable polymer and thus the addition of hyaluronidase resulted in a faster weight loss of AHA-g-PNIPAAm copolymer. Both the AHA-g-PNIPAAm-28 and AHA-g-PNIPAAm-53 hydrogels demonstrated a significant mass loss exceeding 40% when incubated in 100U/ml hyaluronidase/PBS at 37°C over 28 days ($p < 0.05$). Enzymatic resistance of AHA-g-PNIPAAm-28 and AHA-g-PNIPAAm-53 copolymers hydrogels was 12.3% and 37.6% after 28 days, respectively.

SEM analysis revealed the microstructure morphologies of freeze-dried AHA-g-PNIPAAm hydrogels before and after PBS incubation at 37°C (Fig. 4). The initial AHA-g-PNIPAAm-28 and AHA-g-PNIPAAm-53 copolymer hydrogels displayed a continuous and porous structure by virtue of the freeze-drying step, resembling other natural macromolecular hydrogel system structures. The pore diameter of the AHA-g-PNIPAAm-28 copolymer hydrogel is in the range of 3–20μm (Fig. 4a), compared to a diameter of 1–10μm pores for the AHA-g-PNIPAAm-53 copolymer hydrogel (Fig. 4d). This difference in pore size indicates that a higher grafting ratio of PNIPAAm results in the formation of smaller pore diameters and tighter network structure in thermosensitive hydrogels, which is likely due to the comparatively different arrangement of chains during freeze-drying procession. After 21d incubation, the structure of AHA-g-PNIPAAm-28 hydrogel was partially changed, but there was no significant influence brought to the AHA-g-PNIPAAm-53 hydrogels structures.

The effect of the grafting PNIPAAm degrees on the gel structures was evidences after enzymatic degradation in 100U/ml hyaluronidase/PBS at 37°C. After 7d and 21d degradation, the AHA-g-PNIPAAm-28 hydrogel resulted in larger pore diameters (Fig. 5a–b), which is likely due to the mass released from the gel matrix. Compared to AHA-g-PNIPAAm-28, the AHA-g-PNIPAAm-53 hydrogel showed a stable morphological structure during enzymatic degradation and the pore diameters changed only slightly (Fig. 5c–d), although the weight loss ratios significantly increased from 7d to 21d ($p < 0.01$).

Fig. 6 indicates the equilibrium swelling ratios of AHA-g-PNIPAAm copolymer hydrogels determined in PBS and DMEM/F12/10%FBS at 37°C. Grafting ratios of PNIPAAm significantly influenced the equilibrium swelling ratio of AHA-g-PNIPAAm copolymer hydrogels, i.e. the equilibrium swelling ratio of AHA-g-PNIPAAm-28 in PBS was 21.5, which was significantly higher than 13.3 of AHA-g-PNIPAAm-53 ($p < 0.05$). The swelling ratio of AHA-g-PNIPAAm hydrogels in DMEM/F12/10%FBS was slightly changed comparing to those of PBS incubation, whereas no significant difference was found between them ($p > 0.05$). The values remained stable up to 28 days during both PBS and DMEM/F12/10%FBS incubation. At the higher weight ratios of PNIPAAm, the matrix gelled more quickly during the experiment, which might be attributable to the presence of stronger hydrophobic interactions among PNIPAAm chains and the complicated entanglement of macromolecular chains [32–33]. The AHA-g-PNIPAAm-28 hydrogels revealed less grafting PNIPAAm and loose structure, consequently increasing the exposure of hydrophilic polymer chains to water molecules at 37°C (above LCST), and significantly leading to faster weight loss and water absorption enhancement.

3.4. Cytocompatibility of hydrogels

Fig. 7a shows the time course of changes in relative DNA content of the cells in AHA-g-PNIPAAm-28 and AHA-g-PNIPAAm-53 hydrogels. DNA content in both hydrogels progressively decreased compared with initial DNA content. The DNA content of the AHA-g-PNIPAAm-28 hydrogels was significantly decreased after 28d of culture ($p<0.05$). As for the AHA-g-PNIPAAm-53 hydrogels, there was no significant change of DNA number in the entire 28 days of culture ($p > 0.05$), but was significantly greater than those of AHA-g-PNIPAAm-28 hydrogel ($p<0.05$) after 28d culture. Macroscopic morphologies of the cultured ASCs/hydrogels matrices were showed to convey some degree of the degradation effect with cell in Fig. 7b.

After FDA/PI staining, the live/dead encapsulated ASCs within hydrogels after 3D culture for 7d and 21d were imaged by CLSM (Fig. 8). Roundly shaped ASCs were uniformly distributed in both the AHA-g-PNIPAAm-28 and AHA-g-PNIPAAm-53 hydrogels. Most of the encapsulated ASCs were shown to survive in copolymer hydrogels after 7d culture. However, a higher number of live cells were observed in the AHA-g-PNIPAAm-53 hydrogels than the AHA-g-PNIPAAm-28 hydrogels after 21d incubation. However, some live cells precipitated from AHA-g-PNIPAAm-28 hydrogels to the bottom of culture plate after 14d, which likely due to the highly porous structure of AHA-g-PNIPAAm-28 hydrogels in the wet state.

SEM images of the encapsulated ASC/hydrogel matrices are presented in Fig. 9. The residing cells within both AHA-g-PNIPAAm-28 and AHA-g-PNIPAAm-53 hydrogels possessed normal spherical morphology. Since the microstructure and high water content are very similar to that of the extracellular matrix of natural tissue, the copolymer hydrogels may preserve the phenotype of ASCs, predicting a maintainable bioactivity for cell survival support.

3.5. In vivo analysis

AHA-g-PNIPAAm-53 copolymer hydrogels were implanted into the dorsal subcutaneous region of athymic nude mice for 5 days to investigate initial *in vivo* biocompatibility. The animal experiments confirmed the availability of *in situ* gel formation after injection. Fig. 10 displays the representative macroscopic images of the AHA-g-PNIPAAm-53 copolymer hydrogels immediately after injection. The original circular shape was maintained after 5 days implantation. Histological cross sections of the implanted hydrogel and nearby tissue are presented in Fig. 11. A significant amount of the hydrogel remained and no infection was observed in the skin and subcutaneous tissues. No cellular infiltrate around the remaining material was seen at 5 days, although longer studies must be conducted to determine whether the implantation will have further effects, including resorption. The evaluation of these biological properties will contribute to a further understanding of applicability of AHA-g-PNIPAAm copolymer hydrogels. As this process of the hydrogel formation is simple, feasible, and usually performed under mild conditions, we believe that such a thermosensitive injectable hydrogels especially with will have potential applications in wound management, tissue engineering, and other related biomedical fields.

4. Conclusions

Thermosensitive copolymers, aminated hyaluronic acid-g-poly(*N*-isopropylacrylamide) (AHA-g-PNIPAAm), were successfully synthesized. The AHA-g-PNIPAAm hydrogels exhibit reversible temperature-responsive soluble-insoluble characteristics with an LCST of ~30°C. The enzymatic degradation, equilibrium swelling, and cytoviability of copolymer hydrogels were dependent upon weight ratios of PNIPAAm. The AHA-g-PNIPAAm hydrogels with a higher grafting PNIPAAm degree showed a lower equilibrium swelling and degradation rate than those of copolymer with a lower grafting PNIPAAm. Encapsulation of human ASCs

demonstrated that the AHA-g-PNIPAAm copolymer hydrogel promoted cell survival and the cells possessed spherical morphology. In addition, the AHA-g-PNIPAAm copolymer hydrogel with 53% PNIPAAm showed promising biocompatibility in preliminary mouse *in vivo* studies. These studies indicate that the thermosensitive AHA-g-PNIPAAm hydrogel may have potential uses in adipose regeneration and other soft tissue engineering applications. Further studies include long-term *in vivo* studies are underway.

Acknowledgments

We thankfully acknowledge the Center for Biologic Imaging for CLSM/SEM, Professor Sachin Velankar and Michael J. Mazur for assistance with rheology experiments, and NIH R01CA114246-01A1 (JPR).

References

1. Drury JL, Mooney DJ. Hydrogels for tissue engineering: scaffold design variables and applications. Biomaterials 2003;24:4337–51. [PubMed: 12922147]
2. Cosgriff-Hernandez E, Mikos AG. New biomaterials as scaffolds for tissue engineering. Pharm Res 2008;25:2345–7. [PubMed: 18607694]
3. Nuttelman CR, Rice MA, Rydholm AE, Salinas CN, Shah DN, Anseth KS. Macromolecular monomers for the synthesis of hydrogel niches and their application in cell encapsulation and tissue engineering. Prog Polym Sci 2008;33:167–79. [PubMed: 19461945]
4. Hou QP, De Bank PA, Shakesheff KM. Injectable scaffolds for tissue regeneration. J Mater Chem 2004;14:1915–23.
5. Pratt AB, Weber FE, Schmoekel HG, Müller R, Hubbell JA. Synthetic extracellular matrices for in situ tissue engineering. Biotechnol Bioeng 2004;86:27–36. [PubMed: 15007838]
6. Hennink WE, van Nostrum CF. Novel crosslinking methods to design hydrogels. Adv Drug Delivery Rev 2002;54:13–36.
7. Klouda L, Mikos AG. Thermoresponsive hydrogels in biomedical applications. Eur J Pharm Biopharm 2008;68:34–45. [PubMed: 17881200]
8. He C, Kim SW, Lee DS. In situ gelling stimuli-sensitive block copolymer hydrogels for drug delivery. J Control Release 2008;127:189–207. [PubMed: 18321604]
9. Jeong B, Kim SW, Bae YH. Thermosensitive sol-gel reversible hydrogels. Adv Drug Delivery Rev 2002;54:37–51.
10. Shimizu T, Yamato M, Isoi Y, Akutsu T, Setomaru T, Abe K, et al. Fabrication of pulsatile cardiac tissue grafts using a novel 3-dimensional cell sheet manipulation technique and temperature-responsive cell culture surfaces. Circ Res 2002;90:40–8.
11. Gan T, Zhang Y, Guan Y. In situ gelation of P(NIPAM-HEMA) microgel dispersion and its applications as injectable 3D cell scaffold. Biomacromolecules 2009;10:1410–5. [PubMed: 19366198]
12. Qiu Y, Park K. Environment-sensitive hydrogels for drug delivery. Adv Drug Delivery Rev 2001;53:321–39.
13. Kim JH, Lee SS, Kim SJ, Lee YM. Rapid temperature/pH response of porous alginate-g-poly(*N*-isopropylacrylamide) hydrogels. Polymer 2002;43:7549–58.
14. Wang LQ, Tu K, Li Y, Zhang J, Jiang L, Zhang Z. Synthesis and characterization of temperature responsive graft copolymers of dextran with poly(*N*-isopropylacrylamide). React Funct Polym 2002;53:19–27.
15. Stile RA, Burghardt WR, Healy KE. Synthesis and characterization of injectable poly(*N*-isopropylacrylamide)-based hydrogels that support tissue formation in vitro. Macromolecules 1999;32:7370–9.
16. Lee SB, Ha DI, Cho SK, Kim SJ, Lee YM. Temperature/pH-sensitive comb-type graft hydrogels composed of chitosan and poly(*N*-isopropylacrylamide). J Appl Polym Sci 2004;92:2612–20.
17. Cho JH, Kim SH, Park KD, Jung MC, Yang WI, Han SW, et al. Chondrogenic differentiation of human mesenchymal stem cells using a thermosensitive poly(*N*-isopropylacrylamide) and water-soluble chitosan copolymer. Biomaterials 2004;25:5743–51. [PubMed: 15147820]

18. Ha DI, Lee SB, Chong MS, Lee YM, Kim SY, Park YH. Preparation of thermo-responsive and injectable hydrogels based on hyaluronic acid and poly(*N*-isopropylacrylamide) and their drug release behaviors. Macromol Res 2006;14:87–93.
19. Guan JJ, Hong Y, Ma ZW, Wagner WR. Protein-reactive, thermoresponsive copolymers with high flexibility and biodegradability. Biomacromolecules 2008;9:1283–92. [PubMed: 18324775]
20. Ohya S, Nakayama Y, Matsuda T. Thermoresponsive artificial extracellular matrix for tissue engineering: hyaluronic acid bioconjugated with poly(*N*-isopropylacrylamide) grafts. Biomacromolecules 2001;2:856–63. [PubMed: 11710042]
21. Ibusuki S, Fujii Y, Iwamoto Y, Matsuda T. Tissue-engineered cartilage using an injectable and in situ gelable thermoresponsive gelatin: fabrication and in vitro performance. Tissue Eng 2003;9:371–84. [PubMed: 12740100]
22. Goa KL, Benfield P. Hyaluronic acid. A review of its pharmacology and use as a surgical aid in ophthalmology, and its therapeutic potential in joint disease and wound healing. Drugs 1994;47:536–66. [PubMed: 7514978]
23. Toole BP. Hyaluronan and its binding proteins, the hyaladherins. Curr Opin Cell Biol 1990;2:839–44. [PubMed: 1707285]
24. Masters KS, Shah DN, Walker G, Leinwand LA, Anseth KS. Designing scaffolds for valvular interstitial cells: cell adhesion and function on naturally derived materials. J Biomed Mater Res 2004;71A:172–80.
25. Leach JB, Bivens KA, Collins CN, Schmidt CE. Development of photocrosslinkable hyaluronic acid polyethylene glycol-peptide composite hydrogels for soft tissue engineering. J Biomed Mater Res 2004;70A:74–82.
26. Park YD, Tirelli N, Hubbell JA. Photopolymerized hyaluronic acid-based hydrogels and interpenetrating networks. Biomaterials 2003;24:893–900. [PubMed: 12504509]
27. Shu XZ, Liu YC, Luo Y, Roberts MC, Prestwich GD. Disulfide cross-linked hyaluronan hydrogels. Biomacromolecules 2002;3:1304–11. [PubMed: 12425669]
28. Tan HP, Chu CR, Payne KA, Marra KG. Synthesis and characterization of injectable in situ forming biodegradable hydrogel for cartilage tissue engineering. Biomaterials 2009;30:2499–506. [PubMed: 19167750]
29. Jia X, Yeo Y, Clifton RJ, Jiao T, Kohane DS, Kobler JB, et al. Hyaluronic acid-based microgels and microgel networks for vocal fold regeneration. Biomacromolecules 2006;7:3336–44. [PubMed: 17154461]
30. Motokawa K, Hahn SK, Nakamura T, Miyamoto H, Shimoboji T. Selectively crosslinked hyaluronic acid hydrogels for sustained release formulation of erythropoietin. J Biomed Mater Res 2006;78A:459–65.
31. Lee JW, Jung MC, Park HD, Park KD, Ryu GH. Synthesis and characterization of thermosensitive chitosan copolymer as a novel biomaterial. J Biomater Sci Polymer Ed 2004;15:1065–79.
32. Wang J, Chen L, Zhao Y, Guo G, Zhang R. Cell adhesion and accelerated detachment on the surface of temperature-sensitive chitosan and poly(*N*-isopropylacrylamide) hydrogels. J Mater Sci: Mater Med 2009;20:583–90. [PubMed: 18853241]
33. Chen JP, Cheng TH. Thermo-responsive chitosan-graft-poly(*N*-isopropylacrylamide) injectable hydrogel for cultivation of chondrocytes and meniscus cells. Macromol Biosci 2006;6:1026–39. [PubMed: 17128421]
34. Gao CY, MÖhwald H, Shen JC. Thermosensitive poly(allylamine)-g-poly(*N*-isopropylacrylamide): synthesis, phase separation and particle formation. Polymer 2005;46:4088–97.
35. Mao ZW, Ma L, Yan J, Yan M, Gao CY, Shen JC. The gene transfection efficiency of thermoresponsive N,N,N-trimethyl chitosan chloride-g-poly(*N*-isopropylacrylamide) copolymer. Biomaterials 2007;28:4488–500. [PubMed: 17640726]
36. Wieland JA, Houchin-Ray TL, Shea LD. Non-viral vector delivery from PEG-hyaluronic acid hydrogels. J Control Release 2007;120:233–41. [PubMed: 17582640]
37. Marra KG, DeFail AJ, Clavijo-Alvarez JA, Badylak SF, Taieb A, Schipper B, Bennett J, Rubin JP. FGF-2 enhances vascularization for adipose tissue engineering. Plast Reconstr Surg 2008;121:1153–64. [PubMed: 18349632]

38. Aksu AE, Rubin JP, Dudas JR, Marra KG. Role of gender and anatomical region on induction of osteogenic differentiation of human adipose-derived stem cells. Ann Plast Surg 2008;60:306–22. [PubMed: 18443514]

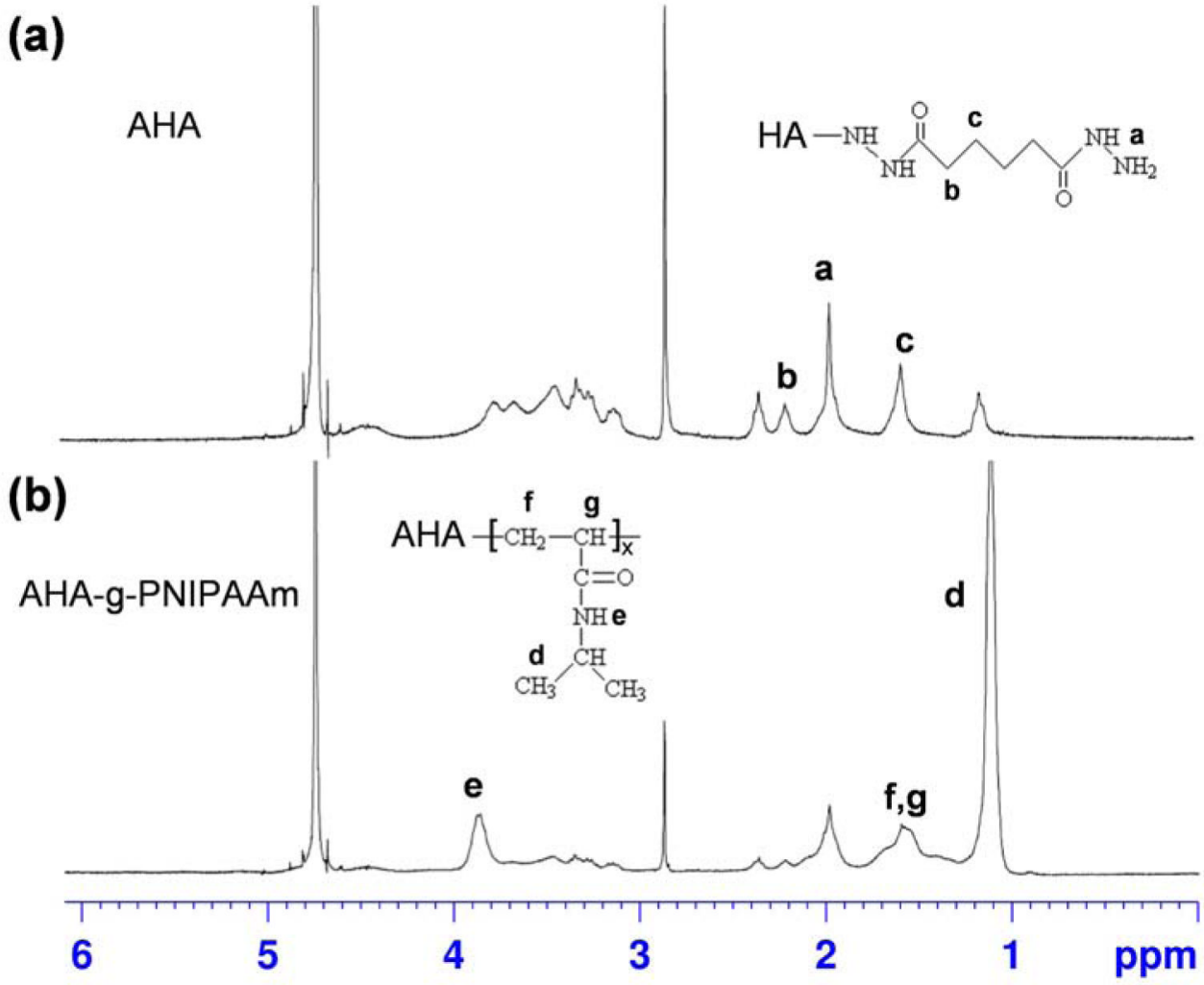

Fig. 1.
^{1}H NMR spectra of (a) AHA and (b) AHA-g-PNIPAAm in D_2O.

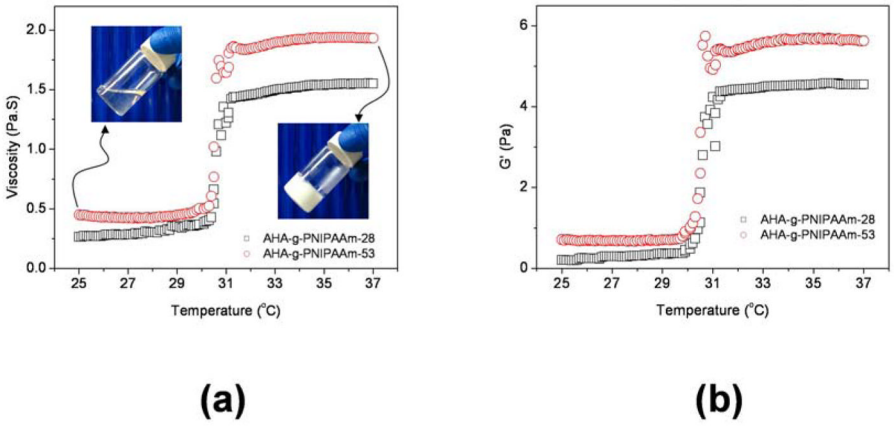

Fig. 2.

Viscosity (a) and storage modulus *G′* (b) of AHA-g-PNIPAAm copolymer with 5 wt % concentration in PBS as a function of temperature. Insets are *in situ* gelation of AHA-g-PNIPAAm hydrogel in PBS.

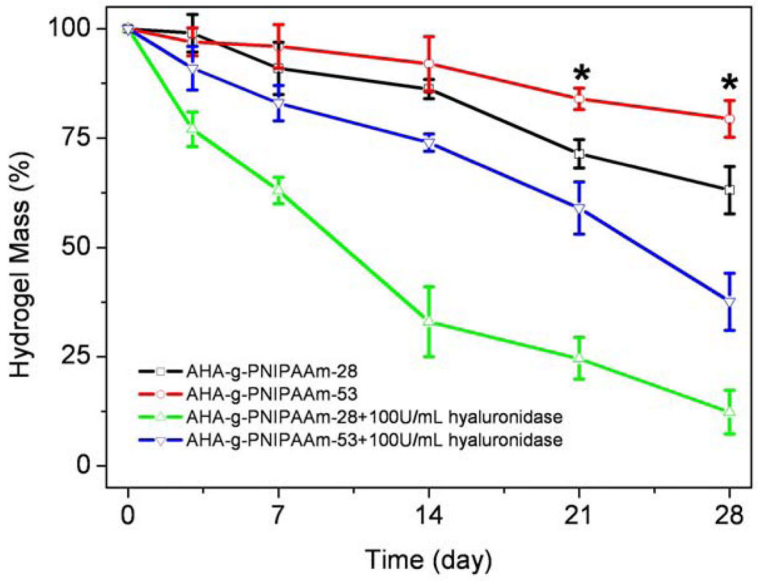

Fig. 3.

Degradation of AHA-g-PNIPAAm copolymer hydrogels in PBS and 100U/ml hyaluronidase/PBS at 37°C with respect to weight loss. Values reported are an average n=5, ± standard deviation.

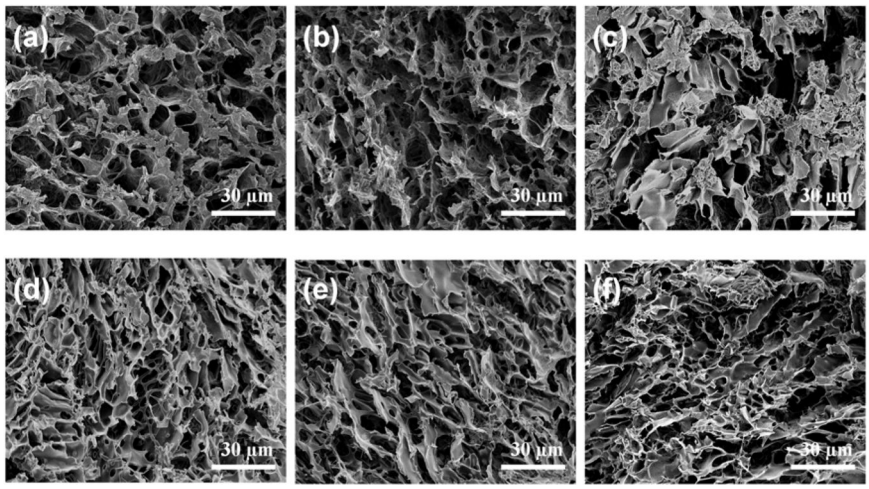

Fig. 4.

SEM images to show the internal structures of AHA-g-PNIPAAm-28 (a–c) and AHA-g-PNIPAAm-53 (d–f) hydrogels before and after incubation in PBS at 37°C for different times. (b, e) and (c, f) are 7 and 21d, respectively.

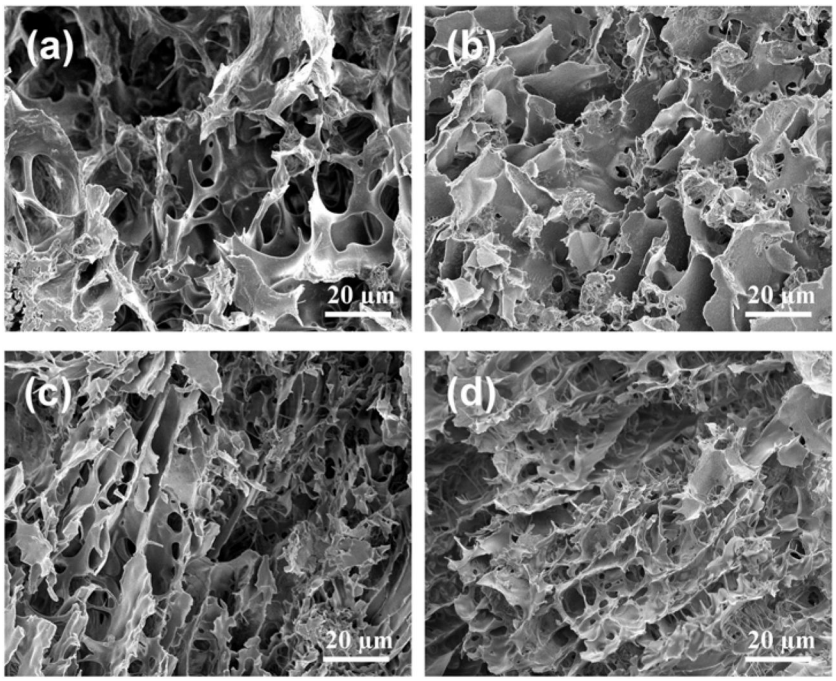

Fig. 5.
SEM images to show the internal structures of AHA-g-PNIPAAm-28 (a–b) and AHA-g-PNIPAAm-53 (c–d) hydrogels after degradation at 37 °C in 100U/ml hyaluronidase/PBS for 7d (a, c) and 21d (b, d).

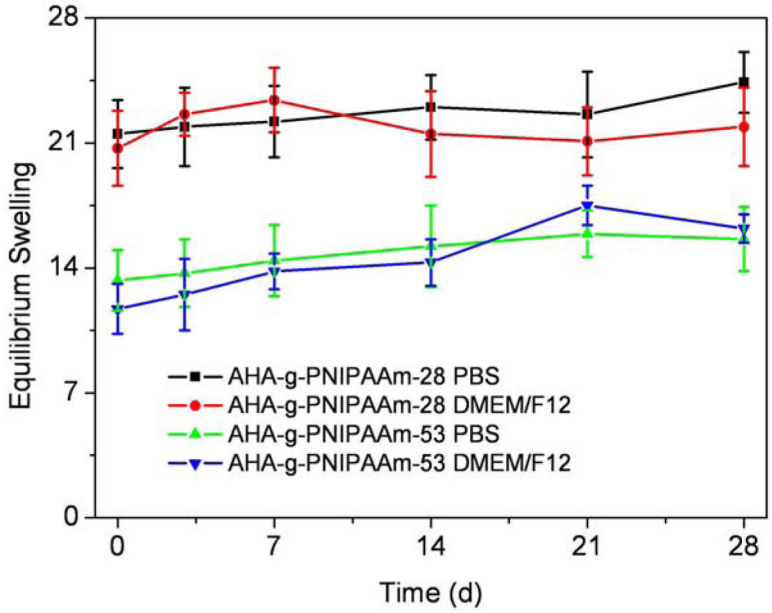

Fig. 6.

Equilibrium swelling ratio of AHA-g-PNIPAAm copolymer hydrogels as a function of incubation time in PBS and DMEM/F12/10%FBS at 37°C. Values reported are an average n=5, ± standard deviation.

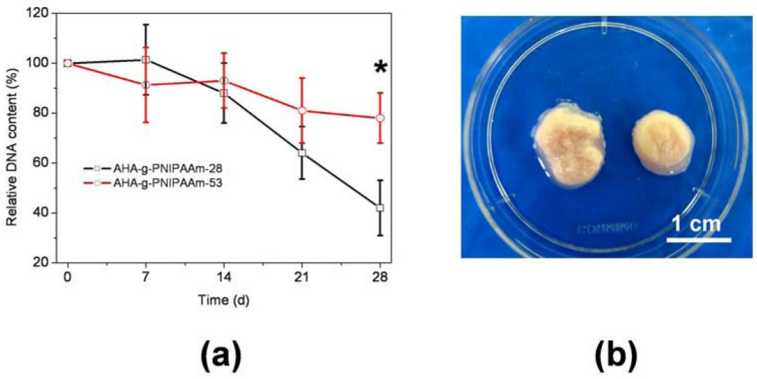

Fig. 7.

(a) DNA contents of encapsulated ASCs in AHA-g-PNIPAAm hydrogels as a function of culture time. Values reported are an average n=3, ± standard deviation. (b) Macroscopic morphologies of cultured ASCs/hydrogels matrices after 21d culture. Left: AHA-g-PNIPAAm-28; Right: AHA-g-PNIPAAm-53.

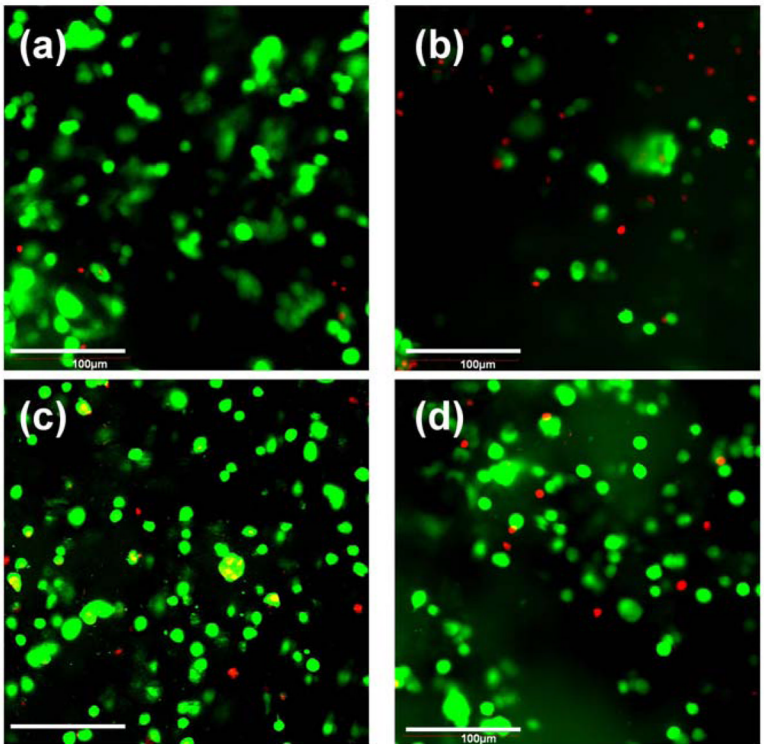

Fig. 8.

CLSM image showing encapsulated ASCs in AHA-g-PNIPAAm-28 (a–b) and AHA-g-PNIPAAm-53 (c–d) hydrogel after 7d (a, c) and 21d (b, d) culture. Cell seeding density: 5×10^6/mL. The live cells were stained with FDA (Green) and the dead cell nuclei were stained with PI (Red).

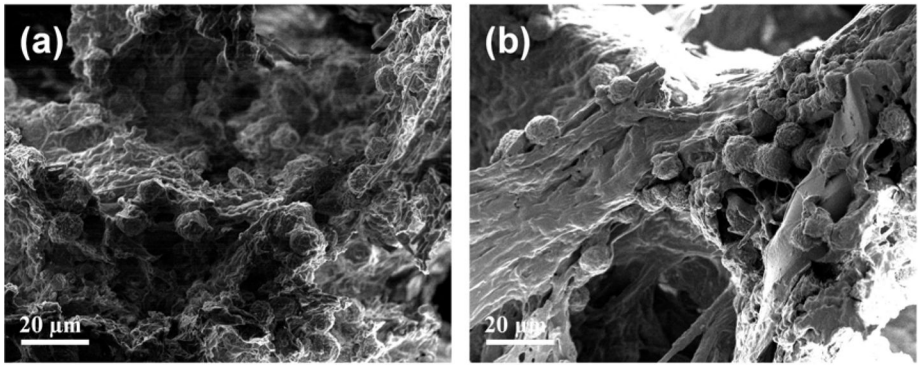

Fig. 9.

SEM image to show the morphology of encapsulated ASCs in AHA-g-PNIPAAm-28 (a) and AHA-g-PNIPAAm-53 (b) hydrogels after 21d culture. Cell seeding density: 5×10^6/mL.

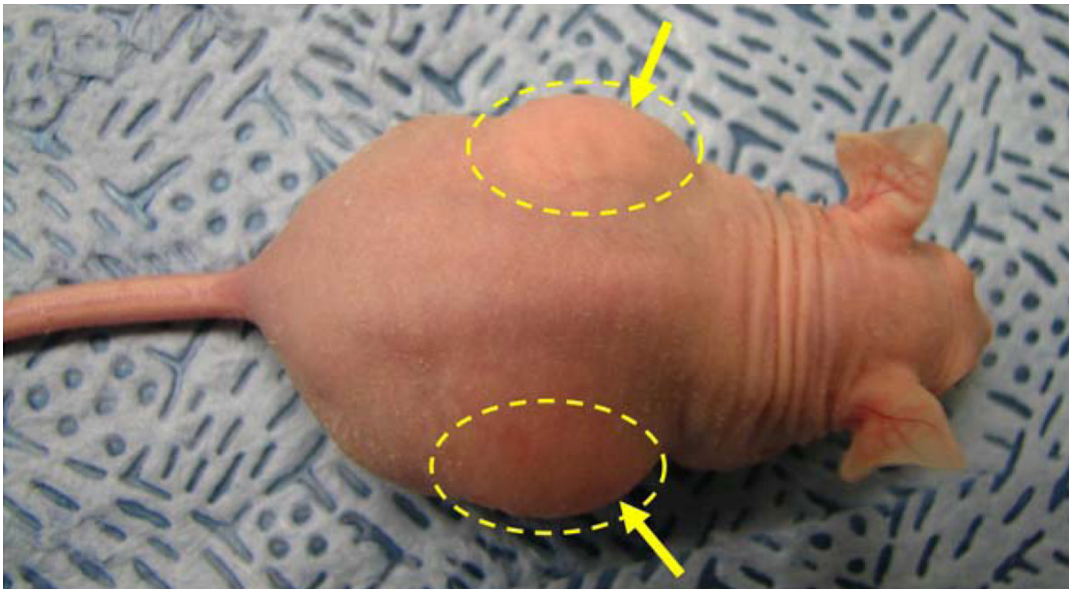

Fig. 10.
Subcutaneous injection of 5 wt% AHA-g-PNIPAAm-53 copolymer hydrogels implants in athymic nude mice after 2h. Yellow arrows denote hydrogel bumps after injection.

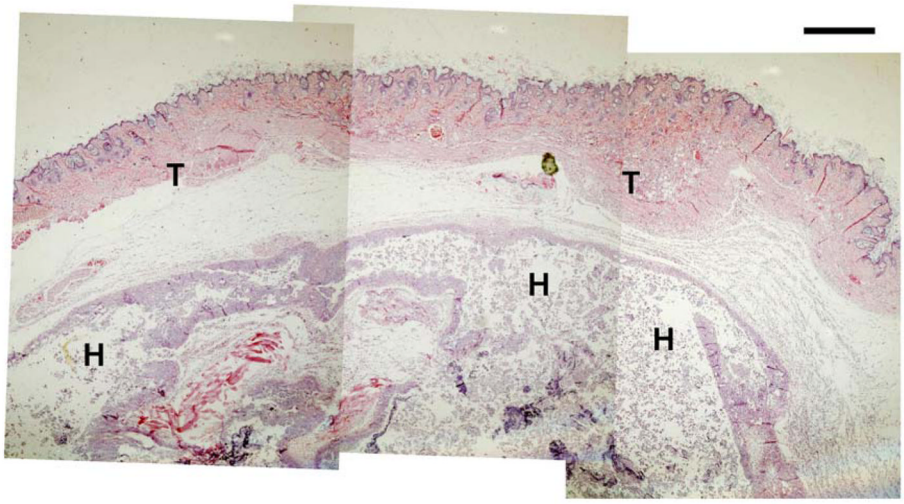

Fig. 11.
H & E staining of AHA-g-PNIPAAm-53 copolymer hydrogels after 5d of implantation. T: tissue; H: hydrogel.

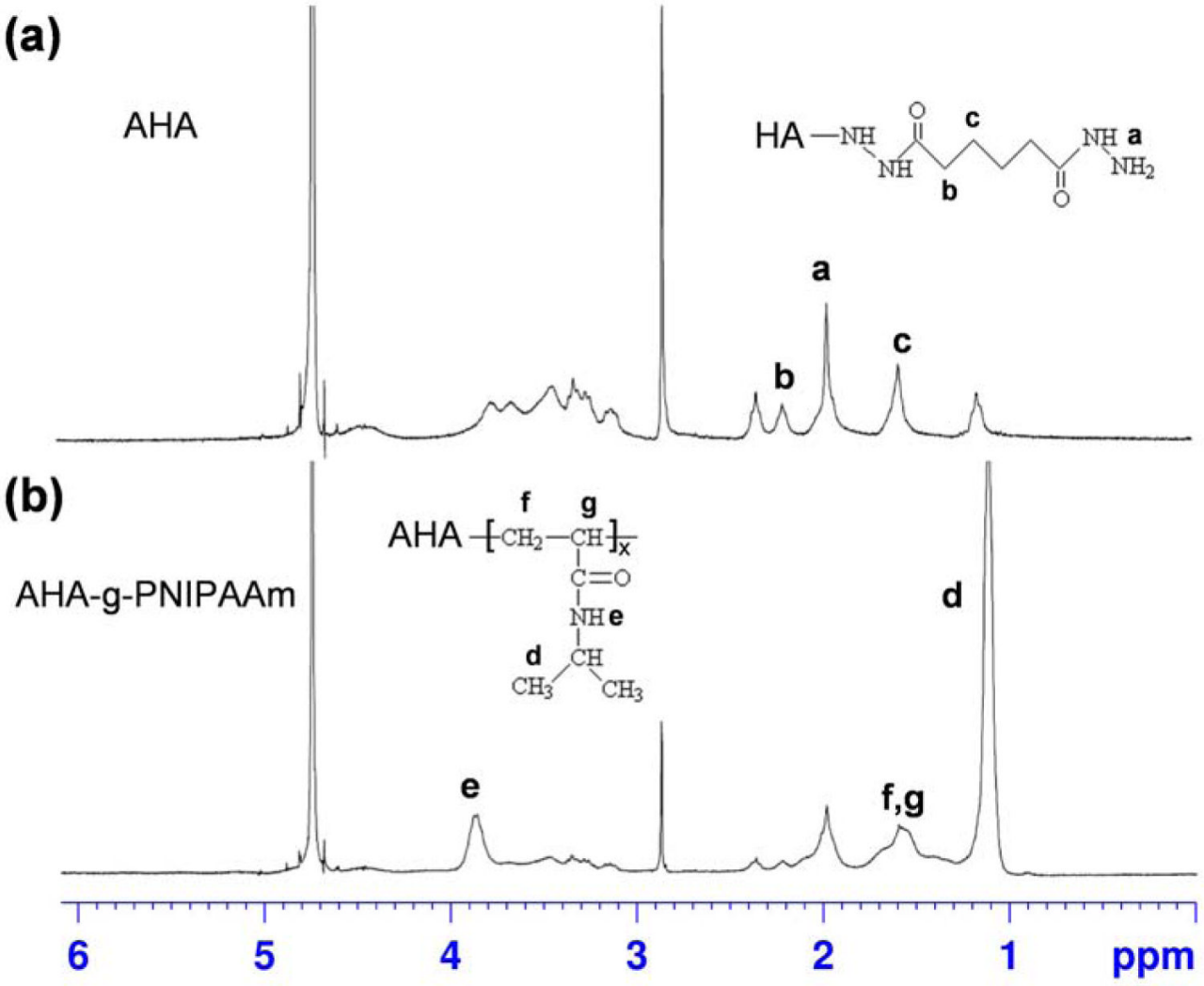

Scheme 1.
Synthetic route of (a) AHA, (b) PNIPAAm-COOH, and (c) AHA-g-PNIPAAm.